INVESTIGATION OF PV SOLAR DEVICES FOR ELECTRICITY PRODUCTION AND HEAT RECOVERY

Davide Del Col, Marco Dai Prè, Matteo Bortolato, Andrea Padovan

Dipartimento di Ingegneria Industriale, Università degli Studi di Padova
Via Venezia, 1 – 35131 Padova – Tel.: +39 049 827 6891 – Fax: +39 049 827 6896
davide.delcol@unipd.it

SUMMARY

The efficiency of a photovoltaic module decreases with increasing cell temperature in crystalline silicon PV cells. The efficiency penalization can be reduced by cooling the photovoltaic module. Moreover, heat can be recovered and used for low temperature applications, such as heating of water in swimming pools and pre-heating of water for domestic use.

This paper reports an investigation of flat plate photovoltaic-thermal (PV/T) devices for the combined production of electrical and thermal energy. Three prototypes have been experimentally characterized and compared. The prototypes consist of a crystalline silicon PV module and a roll-bond canalized panel, made of aluminium, which is applied to the back side of the module and used as heat exchanger. The three PV/T devices differ for the way the roll-bond heat exchanger is applied to the module.

Measurements of thermal and electrical efficiency are reported. The experimental results have been used to validate a numerical model, which is able to predict the thermal and electrical performance of the PV/T devices. The model represents a useful tool to investigate the performance when varying the operating conditions and for further efficiency improvement.

The thermal and electrical efficiency curves are then used for simulating the yearly production of electrical energy and heat of a PV/T system, starting from a database of solar irradiance and ambient air temperature. The model can predict the performance as a function of various operating modes: PV module working with no active cooling, active cooling of the PV module without effective heat recovery and cooling for cogeneration of electricity and heat. Some simulations are reported to discuss the capability of flat-plate PV/T devices in Italy.

INTRODUCTION

Renewable energy sources and energy efficiency are key points to meet the environmental objectives in energy production and utilization. The use of solar energy systems is growing; particularly, the installation of photovoltaic (PV) modules has exhibited a rapid increase in the last years. Photovoltaic modules convert the solar radiation energy flux in electric power. During normal operation, the efficiency of a crystalline silicon PV cell decreases with increasing temperature of the cell. This penalization is significant especially in summer months, when the availability of solar radiation energy is higher and the ambient temperature is higher too. The efficiency decrease can be reduced by cooling the PV module. Moreover, heat can be recovered and used for low temperature applications, such as heating of water for swimming pools and pre-heating of water for domestic use. Therefore, the development of solar devices for the combined production of electrical and thermal energy (PV/T) can be a valid solution to increase the total efficiency.

Two main families of PV/T systems exist. In the first one, named in this work as PV/T collector, the design of the device is similar to that of solar collectors, with the difference that PV cells are located on the absorber plate: an air gap exists between the PV cells and the transparent cover. This solution allows to reduce the heat losses on the front part of the panel, but the PV cells are subjected to more critical operating conditions, as discussed for example by Busato et al. [1]. In the second type, named here as PV/T module, a heat exchanger is applied to the back side of a photovoltaic module. A large number of works is available in the literature on the PV/T collector types, such as for instance the recent papers by Dupeyrat [2], [3], whereas few papers have addressed the optimization of the design of the second type of systems.

In this work three prototypes of PV/T hybrid modules have been characterized and compared. The prototypes consist of a PV crystalline silicon module and a roll-bond canalized panel, made of aluminium, which is applied to the back side of the module and used as heat exchanger. The three PV/T devices differ for the application of the roll-bond heat exchanger to the module. In the first prototype, the roll-bond panel is glued to the back side of the PV module and an insulation layer of 1.5 cm of polyurethane is added for reducing the heat losses from the heat exchanger to ambient air in the rear part. In the second prototype, the roll-bond heat exchanger is mechanically applied to the back side the PV module by means of springs. No insulation layer is used to cover the roll-bond panel. Finally, the third prototype is built by a unique lamination process, in which the roll-bond sheet is added to the multilayer components of the PV module (glass, EVA, PV cells, EVA, backsheet, EVA, roll-bond). The laminated device

is not insulated in the rear part. All the devices have an aperture area of 1.6 m^2. A scheme of the tested devices is reported in Figure 1.

The first and third device have the same pattern of channels in the roll-bond heat exchanger, characterized by a serpentine arrangement, while the second prototype presents parallel channels. In the roll-bond panel the channels for the liquid are integrated in the plate. It is expected that the use of the roll-bond panel can provide a more uniform temperature distribution on the PV cells and a higher heat transfer efficiency as compared to sheet-and-tube absorbers. For instance, Del Col et al. [4] showed that in the case of solar collectors the roll-bond absorber provides a higher performance than the sheet-and-tube absorber, due to the more efficient heat transfer from the plate to the water inside the channels. Besides, the roll bond panel has a configuration adequate to be laminated with the PV module and this can allow building the device with a unique process. An example of lamination of PV cells with a roll-bond panel is reported by Dupeyrat et al. [2], [3] in the case of the PV/T collector type.

The present paper reports experimental measurements of thermal and electrical efficiency for the three prototypes of PV/T modules described above. The experimental results are discussed and used to validate a new numerical model, which is able to predict the thermal and electrical performance of the PV/T devices.

The thermal and electrical efficiency curves are used for simulating the yearly production of electrical energy and heat of a PV/T hybrid system, starting from a database of solar irradiance and ambient air temperature. The model can predict the performance as a function of various operating modes: no cooling of the PV module, cooling of the PV module without heat recovery and cogeneration of electrical energy and heat. Some simulations are reported to discuss the capability of flat-plate PV/T devices.

EXPERIMENTAL TESTS

Tests have been run for the three PV/T prototypes to measure the thermal and electrical efficiency. The experimental apparatus is located at the laboratory of solar energy conversion at the University of Padova, Italy. The test facility has been set up to measure the efficiency of solar collectors in agreement with the test methods described in the European standard EN 12975-2 [5] (Zambolin and Del Col [6]). It includes a hydraulic loop and the instrumentation for the measurement of fluid flow rate, inlet and outlet fluid temperature, solar irradiance, wind speed and ambient air temperature. The PV/T modules are oriented 10° south-west and the tilt angle is set to meet the incidence angle requirement of the standard EN 12975-2 [5]. For the laminated module and the PV/T device mechanically connected, the tests have been run during spring and the tilt angle was set at 45°. In the case of the glued and insulated device the tests have been run during summer and the tilt angle was set at 30°.

The working fluid used in the experimental apparatus is water. A Coriolis effect flow meter is used to measure the water flow rate. The liquid temperature at the inlet and outlet of each module is measured by platinum resistance thermometers (RTDs). Another platinum resistance thermometer measures the ambient air temperature and an anemometer measures the air speed on the horizontal plane.

A Kipp&Zonen CM11 pyranometer, classified as secondary standard, is mounted on the plane of the module to measure the global solar irradiance. A Kipp&Zonen CHP1 pyrheliometer measures the normal beam irradiance; the direct irradiance on the tilted plane of the module is then obtained as reported in Duffie and Beckman [7]. Such instrumentation also allows determining the diffuse fraction on the plane of the modules, which is a parameter to be checked.

Tests have been run under steady-state conditions, following the method described in the standard EN 12975-2 [5]. A water flow rate equal to 0.02 kg/s per square meter of aperture area has been imposed.

Efficiency data have been measured at different values of inlet water temperature. The thermal efficiency is obtained as the ratio of the useful heat flow rate gained by water and the solar power incident on the aperture area:

$$\eta_{th} = \frac{q_u}{G \cdot A} = \frac{m_w \cdot c_p \cdot (T_{out} - T_{in})}{G \cdot A} \quad (1)$$

where q_u is the useful heat flow rate, G is the irradiance on the plane of the module, A is the aperture area of the module, m_w is the water mass flow rate, T_{in} and T_{out} are the inlet and outlet water temperatures.

Efficiency data points are presented in graphs as a function of the reduced temperature difference, defined as:

$$T^*_m = \frac{\frac{T_{in} + T_{out}}{2} - T_{amb}}{G} \quad (2)$$

where T_{amb} is the ambient air temperature.

For the laminated module and the glued and insulated module, the thermal efficiency is measured both without electric load and with an electric load corresponding to the maximum power point. For the mechanically connected device, the thermal characterization has been done only without electric load.

The electrical efficiency has been measured using a I-V curve tracer by EKO Instruments. This instrument provides the I-V curve of the module, so it is possible to determine the maximum electrical power produced, P_{max}. Each measurement requires about 3 seconds, and there are two measurements every minute. The electrical efficiency is:

$$\eta_{el} = \frac{P_{max}}{G \cdot A} \quad (3)$$

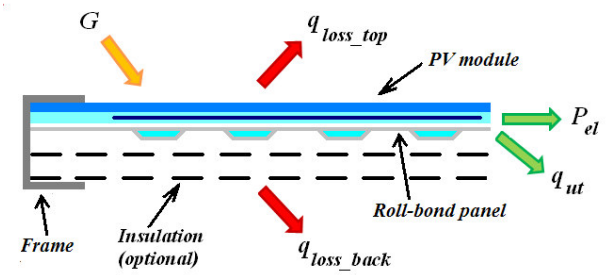

Figure 1. Schematic view of the energy fluxes in the PV/T devices.

NUMERICAL MODEL

In this section the numerical model developed to characterize the electrical and thermal performance of the PV/T modules is described. A 1D approach is adopted in the model, following the findings of Zondag et al. [8], who demonstrated that a simple 1D model can be as effective as the more complicated 2D or 3D models for the prediction of the efficiency curves and the annual yield of a PV/T module. The energy fluxes, considered in the energy balance of the PV/T device, are shown in Figure 1. The model calculates the useful heat flow rate q_u, the electrical power P_{el} and an average temperature for each layer of the PV/T module. The input parameters are: irradiance on the plane of the module G, ambient air temperature T_{amb}, inlet temperature of working fluid T_{in}, flow rate of working fluid m_w and sun spatial coordinates. This model predicts the thermal efficiency in open circuit condition or on load condition.

The heat balance in the PV/T module gives the thermal power absorbed by the roll-bond plate:

$$q_{cell-abs} = G \cdot A \cdot (\tau\alpha)_{eff} - q_{loss\_top} \quad (4)$$

where the term $(\tau\alpha)_{eff}$ is calculated as:

$$(\tau\alpha)_{eff} = \tau_g \cdot \left[\alpha_c \cdot p + \alpha_b \cdot (1-p)\right] - \eta_{el} \quad (5)$$

The glass transmittance τ_g is calculated as reported in Duffie and Beckman [7], neglecting the effect of the absorptance of the glass and considering a refractive index of 1.53. The terms α_c and α_b are the absorptance of PV cells and backsheet respectively, p is the packing factor of the module, which is the ratio of the PV cells total surface to the aperture area. In open circuit conditions, the electrical efficiency, η_{el}, is set equal to zero, while when the electric load is connected it is calculated as reported in Zondag [9]:

$$\eta_{el} = \eta_{ref} \cdot \left[1 - b \cdot (T_{cell} - T_{ref})\right] \quad (6)$$

where η_{ref} is the electrical efficiency of the module at the standard STC conditions (25 °C of PV cell temperature, 1000 W/m^2 of irradiance and 1.5 air mass), b is the temperature coefficient of the module, T_{cell} is the average temperature of the PV cell and T_{ref} is the reference temperature equal to 298.15 K (25 °C). The heat flow rate lost from the glass cover to the ambient air is calculated as:

$$q_{loss\_top} = A \cdot \left(h_{rad\_top} + h_{conv\_top}\right) \cdot \left(T_{cover} - T_{amb}\right) \quad (7)$$

with

$$h_{rad\_top} = \varepsilon_g \cdot \sigma \cdot \frac{\left(T_{cover}^{\ 4} - T_{sky}^{\ 4}\right)}{T_{cover} - T_{amb}} \quad (8)$$

$$h_{conv\_top} = 1.247 \cdot \left[\left(T_{cover} - T_{amb}\right) \cdot \cos\theta\right]^{1/3} + 2.658 \cdot v \quad (9)$$

where ε_g is the emittance of the glass cover, σ is the Stefan-Boltzmann constant, T_{cover} is the average temperature of the glass cover of the PV module, T_{amb} is the ambient air temperature, T_{sky} is the equivalent sky temperature, calculated using the Whillier equation for clear sky ($T_{sky} = T_{amb} - 6$); the heat transfer coefficient between the glass cover of the PV module and the ambient air is calculated with Eq. (9) as reported in Stultz and Wen [10], where θ is the tilt angle of the module and v is the wind speed. A value of wind speed equal to 1.5 m/s has been used in the simulations, which is very close to the average wind speed measured during the experimental tests for the present modules.

The heat flow rate transferred from the PV cells to the absorber plate equals the sum of the useful heat flow rate gained by the fluid and the dissipations towards the back side of the device:

$$q_{cell-abs} = q_u + q_{loss\_back} \quad (10)$$

The heat loss from the absorber plate towards the rear of the module is calculated as:

$$q_{loss\_back} = A \cdot \left(h_{rad\_back} + h_{conv\_back}\right) \cdot \left(T_{abs} - T_{amb}\right) \quad (11)$$

in the case of laminated module and mechanically connected module, and:

$$q_{loss\_back} = A \cdot h_{cond\_ins} \cdot \left(T_{abs} - T_{amb}\right) \quad (12)$$

in the case of glued and insulated module. The heat transfer coefficients in Eq. (11) and Eq. (12) are calculated as:

$$h_{rad\_back} = \varepsilon_{abs} \cdot \sigma \cdot \frac{\left(T_{abs}^{\ 4} - T_{amb}^{\ 4}\right)}{T_{abs} - T_{amb}} \quad (13)$$

$$h_{conv\_back} = 1.247 \cdot \left[\left(T_{abs} - T_{amb}\right) \cdot \cos\theta\right]^{1/3} + 2.658 \cdot v \quad (14)$$

$$h_{cond\_ins} = \frac{\lambda_{ins}}{s_{ins}} \quad (15)$$

where T_{abs} is the average temperature of the absorber plate, ε_{abs} is the emittance of the absorber plate, λ_{ins} is the thermal conductivity of the back insulation layer, s_{ins} is the thickness of the insulation layer.

The model is based on an iterative process, which starts by assuming an initial value of temperature of the PV cells. The model then calculates the heat dissipation from the glass cover to the ambient with Eq. (7) and the heat flux transferred to the absorber with Eq. (4). A subroutine calculates the temperature of the absorber plate and the useful heat flux to the working fluid by means of an iterative process, which ends when Eq. (10) is satisfied. The new temperature of the PV cells is obtained from an energy balance between the PV cells and the roll-bond plate. Conduction heat transfer between the glass cover and the absorber plate is assumed and the thermal resistance of the different layers is considered. In the case of the glued and thermally insulated PV/T module the layers

consist of: glass cover, a first EVA layer, a second EVA layer, polyester based backsheet, glue, roll-bond plate; the thermal resistance of the layer of PV cells is neglected due to the higher value of the silicon thermal conductivity as compared to the other terms. In the case of the mechanically connected module the layers are the same as the glued and thermally insulated device with the exception of the glue layer; a small air gap is assumed between the backsheet and the absorber plate, in order to take into account the non-uniform contact between the plate and the module. In the case of the laminated module the layers are again the same as the glued and thermally insulated device with the exception of the glue layer, which is replaced with an EVA layer to ensure the contact between the backsheet and the roll-bond plate.

The effect of the thermal capacitance of the various layers of the device is neglected, thus the model works in steady-state conditions.

The outlet water temperature is obtained from the useful heat flow rate transferred to the fluid:

$$q_u = m_w \cdot c_p \cdot \left(T_{out} - T_{in}\right) \tag{16}$$

while the electric power produced is:

$$P_{el} = G \cdot A \cdot \eta_{el} \tag{17}$$

EXPERIMENTAL AND NUMERICAL RESULTS

The results of experimental tests and numerical simulations are reported in graphs that show the electrical and thermal efficiency as a function of the reduced temperature difference. Each experimental point of thermal efficiency is measured during a time interval of 10 minutes. The experimental uncertainties (with 95% confidence interval) of the measured values of thermal efficiency and reduced temperature difference are determined following the procedure described in ISO [11] and in Kratzenberg et al. [12] and are reported in the graphs.

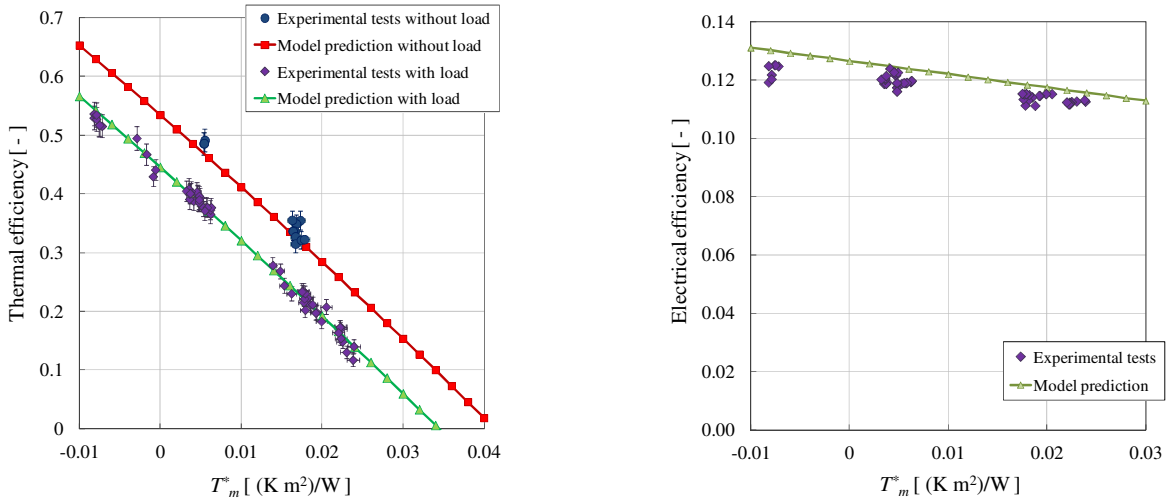

Figure 2. Glued and insulated PV/T module: thermal efficiency (left) and electrical efficiency (right).

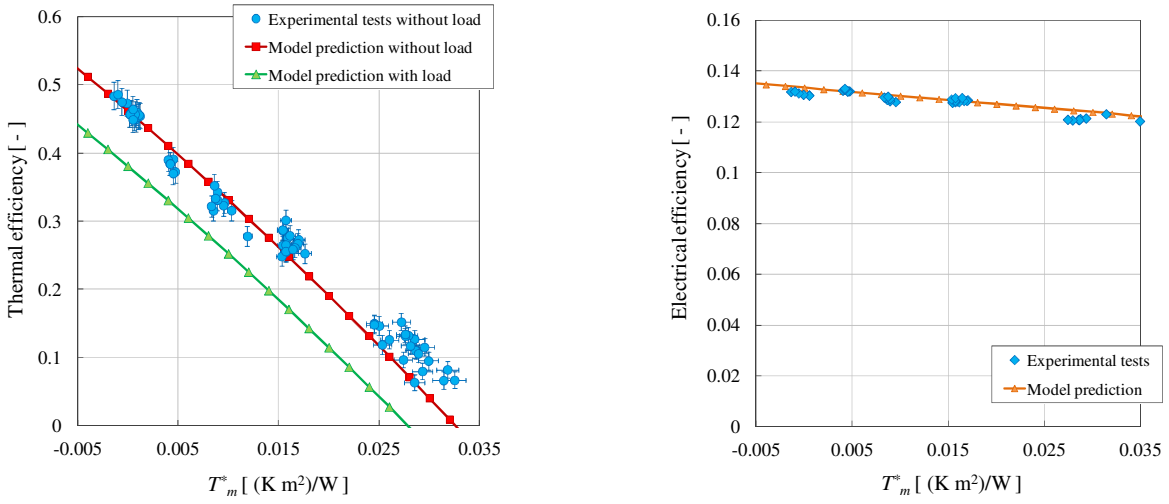

Figure 3. Mechanically connected PV/T module: thermal efficiency (left) and electrical efficiency (right).

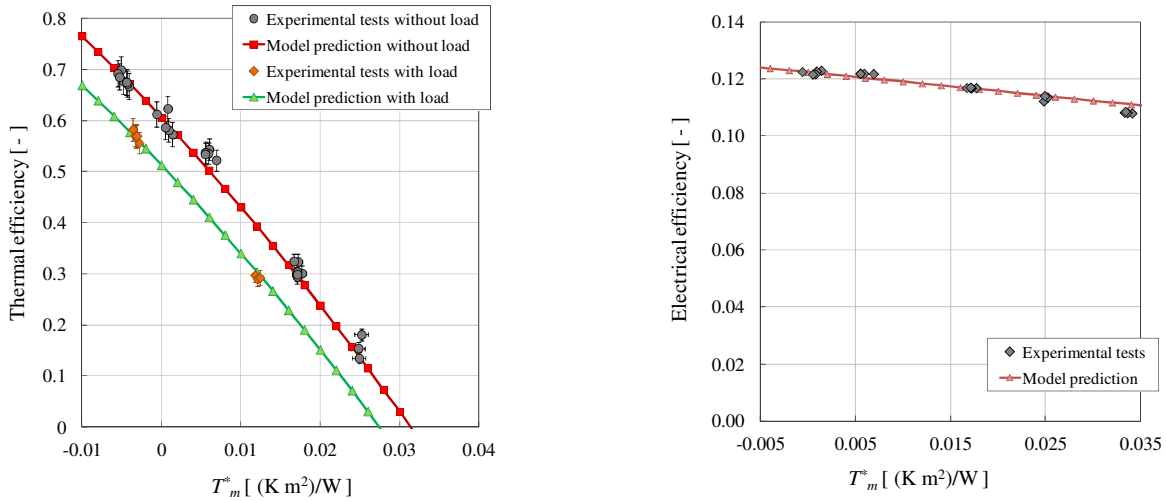

Figure 4. Laminated PV/T module: thermal efficiency (left) and electrical efficiency (right).

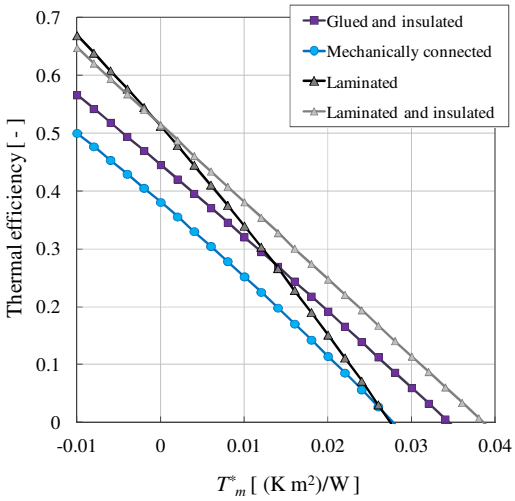

Figure 5. Comparison of thermal efficiency for different PV/T modules (from numerical simulations).

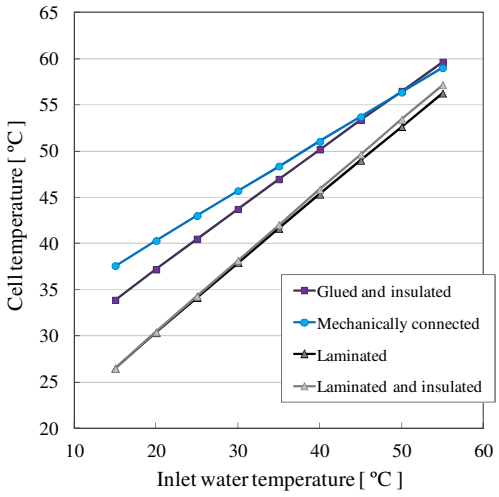

Figure 6. PV cell temperature vs. inlet water temperature for different PV/T modules (from numerical simulations).

The simulations have been performed in the cases of open circuit and with electric load corresponding to the maximum power point condition. The two conditions are characterized by different values of thermal efficiency and PV cell temperature. The cell temperature is higher in open circuit condition. For each module, the calculated efficiency is obtained with 1000 W/m^2 irradiance on the plane of the module (value recommended by EN 12975-2 [5] for steady-state thermal characterization) and ambient conditions equal to the average conditions observed during the tests.

The graphs of Figure 2 show the results for the glued and insulated PV/T module. The thermal efficiency has been measured in open circuit conditions and under maximum power point electric load. High values of reduced temperature difference are associated with low irradiance or high values of fluid to ambient temperature difference. The graph of electrical efficiency reports the experimental points and the model prediction with an electric load at maximum power point conditions.

Figure 3 reports the results for the mechanically connected PV/T module. The thermal efficiency has been measured only in open circuit conditions. The graph of electrical efficiency reports the experimental data points and the model's predictions obtained with the temperature of PV cells without electric load. The electrical efficiency is measured with the I-V curve tracer and the measurement lasts about 3 seconds, with two acquisitions every minute. Therefore for most of the time the module is in open circuit conditions; from the thermal point of view, the short time when the module circuit is closed is not long enough to reach the operating cell temperature. Please note that the electrical efficiency calculated by the model is closely related to the cell temperature as reported in Eq. (6) and that the cell temperature is different if calculated with or without an electric load connected to the module.

The results for the laminated PV/T module are reported in Figure 4. In this case the thermal efficiency has been measured in open circuit condition and in maximum power point electric load. The graph of electrical efficiency reports the experimental data points and the model's predictions obtained under the assumption of open circuit, for the same reason described for the mechanically connected PV/T module.

The thermal efficiency is higher in open circuit condition than on load condition: from Eq. (5), if $\eta_{el} = 0$, the heat flux transferred from the PV cells to the absorber plate is higher and then, from Eq. (10), the useful heat flux q_{ut} is higher.

After validation, the model has been used to compare the performance of the different PV/T modules. The graph of Figure 5 reports the thermal efficiency, calculated by the model at the maximum electric power point, for the three prototypes and for a laminated PV/T module with the same characteristics of the laminated device but provided with a rear thermal insulation (about 1.5 cm of polyurethane). The graph shows how, with low values of reduced temperature difference, the laminated devices exhibit a higher thermal efficiency than the other types of PV/T modules, because of the low thermal resistance between PV cells and absorber plate. When the reduced temperature difference increases, the rear insulation plays a significant role and the device with the higher thermal efficiency is the laminated one with insulation.

Figure 6 reports the trends of the PV cell temperature for the different devices. The simulations have been run with an ambient air temperature of 20 °C and a global irradiance of 1000 W/m^2, at varying the inlet water temperature. The graph shows how the laminated modules can provide a better cooling of the cells as compared to the other two systems. Moreover, experimental observations performed with an infrared camera have shown a highly uniform temperature of the PV cells in the case of the laminated module.

ASSESSMENT OF ANNUAL PRODUCTION OF ELECTRICAL ENERGY AND HEAT

Simulations of annual yield of electrical energy and heat by a PV/T module have been performed for Padova (45.4°N, 11.9°E) and Catania (37.5°N, 15.1°E), starting from a database of solar radiation on the horizontal plane and ambient air temperature. The Climate-SAF database, by PVGIS [13], has been used. This database provides the daily profile of global and diffuse irradiance and ambient air temperature, with a time step of fifteen minutes, for a representative day of each month of the year. The latitude of the location under consideration and the tilt angle of the installation are required as input data. The inclinations of the modules are 34° for Padova and 30° for Catania. The global irradiance on the tilted plane of the module is calculated using the HDKR model by Reindl et al. [14]. The total amount of monthly and annual irradiation on the unitary surface of the module is then obtained. The HDKR model has been chosen, because it has a good accuracy in the estimation of the irradiance on tilted planes, as shown by Padovan and Del Col [15]. The geometrical and thermal properties of the component materials of the PV/T device are implemented. For these simulations, the glued and thermally insulated PV/T device has been considered.

A parameter, named *OCT* (operating cell temperature) is introduced in the calculations. This parameter is the estimated working temperature of the PV cells under the same boundary conditions as defined for *NOCT* (800 W/m^2 irradiance, 20 °C ambient temperature, 1 m/s wind speed), but considering different heat transfer modes in the back side of the module. The *OCT* is calculated from an energy balance on the photovoltaic module. Two cases are considered: natural convection heat transfer on the rear part of the module, which provides an *OCT* equal to about 50 °C, and no heat loss from the rear part of the module, which provides an *OCT* equal to around 60 °C. When forced convection heat transfer is considered, with a wind speed of 1 m/s, on the front and back sides of the photovoltaic module, the estimated temperature is equal to the *NOCT* as provided by the manufacturer of the photovoltaic module (45 °C in this case). From the *OCT*, it is possible to determine the real operating temperature of the PV module and thus the electrical efficiency corresponding to each database condition, when convection heat transfer or adiabatic behaviour occurs on the back side of the module.

The heat transfer in the roll-bond panel is modelled to evaluate the effect of PV cooling by running water inside the channels at an inlet temperature of 20 °C and to assess the possibility of a cogeneration by running water at an inlet temperature of 40 °C. The water mass flux is equal to 0.02 kg/(m^2 s) is assumed. In the two different cooling strategies the water is pumped to the roll-bond heat exchanger only when the PV cell temperature is higher than the inlet water temperature and if the global irradiance on the tilted plane of the module is at least 100 W/m^2. Provided that the PV cell is hotter than the inlet water, the thermal efficiency is calculated from the corresponding curve of the PV/T module under investigation. Once the heat flow rate transferred to the water is known, the water outlet temperature is computed and compared with the water inlet temperature: if the temperature gain is less than 1 K, no water flow is considered. When cooling occurs, the total daily amount of heat produced by the unitary surface of the module, the daily number of hours of heat production and the daily electrical energy yield are obtained. When there is no cooling, only the electrical energy yield is calculated.

The results of the simulations report four different cases: PV module characterized by *OCT* = 50 °C, PV module characterized by *OCT* = 60 °C, hybrid PV/T device with cooling by water at inlet temperature of 20 °C and hybrid PV/T device with cooling by water at inlet temperature of 40 °C. In the cases of PV module, with *OCT* 50 °C or 60 °C, the cell temperature is calculated as:

$$T_{cell} = T_{amb} + \frac{OCT - 20}{800} \cdot G \tag{18}$$

where G and T_{amb} are the irradiance and the ambient temperature provided by the PVGIS database. In the case of hybrid PV/T device, the cell temperature is calculated from the heat balance in the module.

Table 1 reports the results for Padova in the case of the glued and insulated PV/T device. When water is introduced at 20 °C, the annual yield of electrical energy increases, depending on the value of *OCT* considered, but there is not heat recovery. When water is introduced at 40 °C, the yield of electrical energy does not change significantly as compared to a PV module, but there is heat recovery, which is considerable from June to August as shown in Figure 7.

The results for Catania are reported in Table 2 and Figure 8: the gain of annual yield of electrical energy obtained by cooling with inlet water temperature at 20 °C as compared to the case of not cooled PV module increases as compared to Padova, because of the higher average ambient temperature in Catania. For the same reason, also the heat recovery increases as compared to Padova and when the water inlet temperature is 40 °C, there is a significant production of thermal energy from May to September.

Table 1. Production of electrical energy in Padova by the glued and thermally insulated PV/T device.

MONTH	Solar energy Database PVGIS Climate-SAF	Electrical energy OCT = 50 °C	Electrical energy OCT = 60 °C	Electrical energy, cooling T_{in} = 20 °C	Electrical energy, cooling T_{in} = 40 °C
	[kWh/m^2]	[kWh/m^2]	[kWh/m^2]	[kWh/m^2]	[kWh/m^2]
January	69.03	9.79	9.62	9.62	9.62
February	100.66	13.93	13.56	13.56	13.56
March	149.97	20.04	19.40	20.84	19.40
April	167.22	21.74	20.98	23.19	20.98
May	194.19	24.32	23.39	26.85	23.94
June	190.36	23.32	22.42	26.22	23.68
July	210.55	25.26	24.16	29.01	26.34
August	193.22	23.43	22.46	26.73	24.26
September	161.79	20.42	19.67	22.56	20.10
October	115.89	15.27	14.86	16.11	14.86
November	73.95	10.16	9.96	9.96	9.96
December	69.29	9.80	9.62	9.62	9.62
TOTAL YEARLY PRODUCTION	**1696.12**	**217.49**	**210.11**	**234.28**	**216.33**
		% gain compared to OCT = 50 °C		**7.72%**	**-0.54%**
		% gain compared to OCT = 60 °C		**11.51%**	**2.96%**

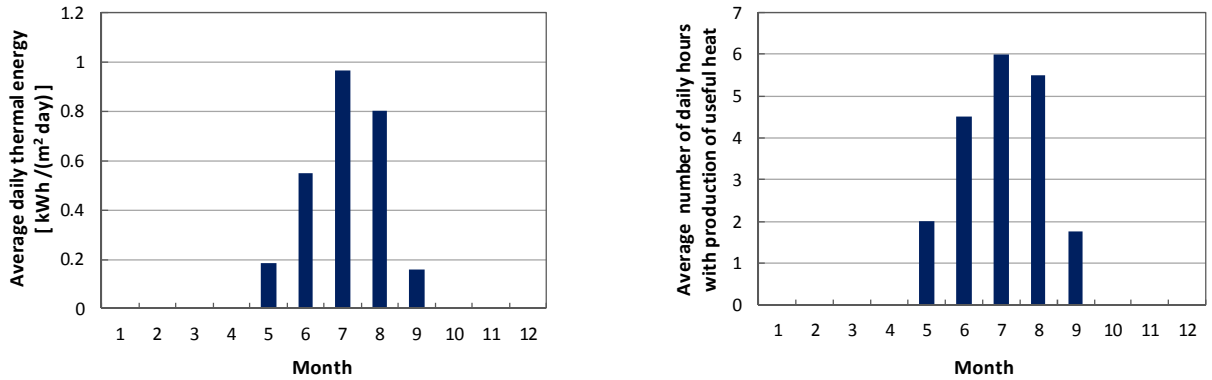

Figure 7. Heat production at 40 °C by the glued and thermally insulated PV/T device in Padova: average daily thermal energy production (left) and average number of daily hours with production of heat (right).

CONCLUSIONS

In this work the experimental and numerical characterization of three types of PV/T modules is presented. The devices consist of a roll-bond canalized panel attached to the back of a photovoltaic module. The prototypes tested differ in the way the roll-bond heat exchanger is connected to the back side of the PV module.

The results have shown that the lamination of the canalized panel with the photovoltaic module in a unique process allows to achieve the higher thermal performance, because it ensures the lower thermal resistance between the PV cells and the aluminium plate: in this case the thermal efficiency is the highest and the PV cells temperature is the lowest among the three solutions investigated.

The numerical model has exhibited a good agreement with the experimental measurements and it is a valid tool for a more comprehensive analysis of the configurations studied.

Simulations of annual production of electrical energy and heat by the glued and thermally insulated PV/T module have been run. For example, a solar collector with an average daily efficiency of 50%, installed in Padova with optimal orientation and inclination, provides a daily heat production of around 3 kWh/m^2 during summer months. To produce the same amount of heat at 40 °C it is necessary a surface of PV/T modules around 3 ÷ 5 times higher. The capability of the PV/T installation increases when considering the case of Catania, due to the higher solar radiation availability and higher values of ambient air temperature.

Table 2. Production of electrical energy in Catania by the glued and thermally insulated PV/T device.

MONTH	Solar energy Database PVGIS Climate-SAF	Electrical energy OCT = 50 °C	Electrical energy OCT = 60 °C	Electrical energy, cooling T_{in} = 20 °C	Electrical energy, cooling T_{in} = 40 °C
	[kWh/m^2]	[kWh/m^2]	[kWh/m^2]	[kWh/m^2]	[kWh/m^2]
January	123.41	16.33	15.81	17.11	15.81
February	129.24	17.03	16.45	18.02	16.45
March	172.91	22.40	21.55	24.09	21.55
April	182.17	23.20	22.28	25.36	22.28
May	207.68	25.61	24.50	28.79	26.06
June	213.46	25.49	24.27	29.49	26.81
July	233.99	27.27	25.80	32.40	29.54
August	225.14	26.27	24.89	31.15	28.40
September	181.98	22.01	21.04	25.23	22.89
October	159.15	19.90	19.14	22.18	19.88
November	124.64	16.14	15.61	17.39	15.61
December	121.38	16.03	15.53	16.91	15.53
TOTAL YEARLY PRODUCTION	**2075.16**	**257.70**	**246.86**	**288.10**	**260.81**
			% gain compared to OCT = 50 °C	**11.80%**	**1.21%**
			% gain compared to OCT = 60 °C	**16.70%**	**5.65%**

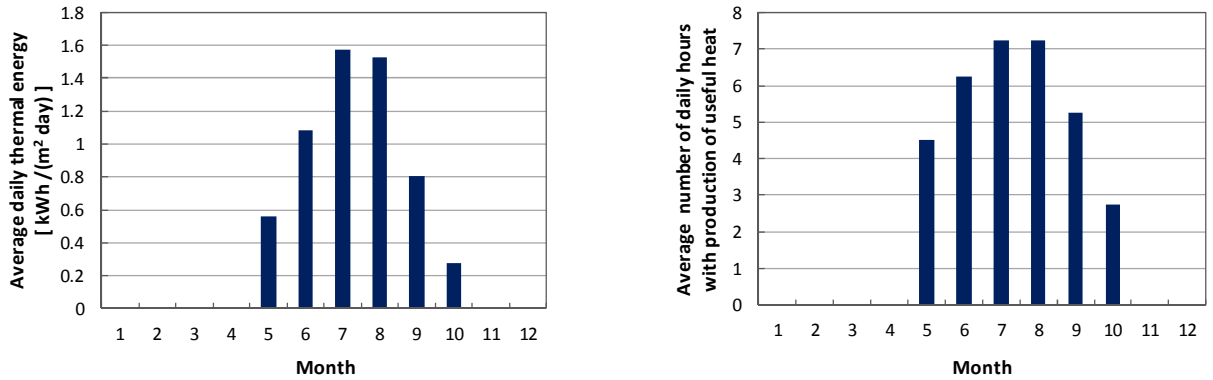

Figure 8. Heat production at 40 °C by the glued and thermally insulated PV/T device in Catania: average daily thermal energy production (left) and average number of daily hours with production of heat (right).

NOMENCLATURE

A	area of the module [m^2]
b	temperature coefficient of the module [1/K]
c_p	specific heat at constant pressure [J/(kg K)]
G	global irradiance on the module plane [W/m^2]
h_{cond_ins}	conduction heat transfer coefficient of the insulation layer [W/(m^2 K)]
h_{conv_back}	convection heat transfer coefficient between absorber plate and ambient air [W/(m^2 K)]
h_{conv_top}	convection heat transfer coefficient between glass cover and ambient air [W/(m^2 K)]
h_{rad_back}	radiation heat transfer coefficient between absorber plate and ambient air [W/(m^2 K)]
h_{rad_top}	radiation heat transfer coefficient between glass cover and ambient air [W/(m^2 K)]
m_w	working fluid flow rate [kg/s]
$NOCT$	normal operating cell temperature [°C]
OCT	operating cell temperature [°C]
p	packing factor [-]
P_{el}	electric power produced [W]
P_{max}	maximum electrical power produced [W]
$q_{cell\text{-}abs}$	heat flow rate from the PV cells to the absorber plate [W]
q_{loss_top}	heat flow rate loss from the glass cover to the ambient air [W]
q_{loss_back}	heat flow rate from the absorber plate to the ambient air [W]
q_u	useful heat flow rate to the fluid [W]
s_{ins}	thickness of the insulation [m]

T^*_m reduced temperature difference [(K m^2)/W]
T_{abs} temperature of the absorber plate [K]
T_{amb} ambient air temperature [K]
T_{cell} temperature of the PV cells [K]
T_{cover} temperature of the glass cover [K]
T_{in} working fluid inlet temperature [K]
T_{out} working fluid outlet temperature [K]
T_{ref} reference STC temperature [K]
T_{sky} equivalent sky temperature [K]
v wind speed [m/s]

Greek symbols

α_b absorptance of backsheet [-]
α_c absorptance of the PV cells [-]
ε_{abs} emittance of the absorber plate [-]
ε_g emittance of the glass cover [-]
η_{el} electrical efficiency of the module [-]
η_{ref} electrical efficiency of the module at STC conditions [-]
η_{th} thermal efficiency of the module [-]
θ tilt angle of the module [°]
λ_{ins} thermal conductivity of the insulation [W/(m K)]
σ Stefan-Boltzmann constant [W/(m^2 K^4)]
$(\tau\alpha)_{eff}$ effective trasmittance absorptance product [-]
τ_g trasmittance of the glass cover [-]

ACKNOWLEDGEMENTS

The authors would like to acknowledge the financial support of the Regione Veneto through the project FSE 2105/1/6/1102/2010 and the support of CGA Technologies Spa, Silfab SpA and Rem srl are also acknowledged.

REFERENCES

1. F. Busato, R. Lazzarin, M. Noro, *Experimental analysis of photovoltaic cogeneration modules*, International Journal of Low Carbon Technologies, 3, pp. 221-224, 2008.

2. P. Dupeyrat, C. Ménézo, M. Rommel, H.-M. Henning, *Efficient single glazed flat plate photovoltaic-thermal hybrid collector for domestic hot water system*, Solar Energy, 85, pp. 1457-1468, 2011.

3. P. Dupeyrat, C. Ménézo, H. Wirth, M. Rommel, *Improvement of PV module optical properties for PV-thermal hybrid collector application*, Solar Energy Materials & Solar Cells, 95, pp. 2028-2036, 2011.

4. D. Del Col, M. Dai Prè, M. Bortolato, A. Padovan, *Experimental characterization of thermal performance of flat plate solar collectors with roll-bond absorbers*, Proc. ISES Solar World Congress, Kassel, Germany, 2011.

5. EN 12975-2, *Thermal solar systems and components - Solar collector - Part 2: Test methods*, CEN, Brussels, 2006.

6. E. Zambolin, D. Del Col, *Experimental analysis of thermal performance of flat plate and evacuated tube solar collectors in stationary standard and daily conditions*, Solar Energy, 85, pp. 1382-1396, 2010.

7. A. Duffie, W. A. Beckman, *Solar engineering of thermal processes*, 3rd ed, Wiley & Sons, New Jersey, 2006.

8. H. A. Zondag, D.W. de Vries, W.G.J. van Helden, R.J.C. van Zolingen, A.A. van Steenhoven, *The yield of different combined PV-thermal collector designs*, Solar Energy, 74, pp. 253-269, 2003.

9. H. A. Zondag, *Flat-plate PV-Thermal collectors and systems: a review*, Renewable and Sustainable Energy Reviews, 12, pp. 891–959, 2008.

10. J. W. Stultz, L. C. Wen, *Thermal performance testing and analysis of photovoltaic modules in natural sunlight*, LSSA Project Task Report 5101-31, Jet Propulsion Laboratory, California Institute of Technology, Pasadena CA, 1977.

11. ISO, *Guide to the Expression of Uncertainty in Measurement*, 1st ed, International Organization for Standardization, Switzerland, 1995.

12. M. G. Kratzenberg, H. G. Beyer, S. Colle, *Uncertainty calculation applied to different regression methods in the quasi-dynamic collector test*, Solar Energy, 80, pp. 1453-1462, 2006.

13. http://re.jrc.ec.europa.eu/pvgis.

14. D. T. Reindl, W. A. Beckman, J. A. Duffie, *Evaluation of hourly tilted surfaces radiation models*, Solar Energy, 45, pp. 9-17, 1990.

15. A. Padovan, D. Del Col, *Measurement and modeling of solar irradiance components on horizontal and tilted planes*, Solar Energy, 84, pp. 2068-2084, 2010.

SOMMARIO

L'efficienza di un modulo fotovoltaico diminuisce al crescere della temperatura delle celle. Il raffreddamento del modulo fotovoltaico può consentire un aumento delle prestazioni. Inoltre, dal raffreddamento del modulo si può recuperare calore, che può essere utilizzato in applicazioni a bassa temperatura, come per esempio il riscaldamento dell'acqua per piscine e il preriscaldamento dell'acqua calda sanitaria. Questa memoria riporta uno studio sperimentale e numerico su dispositivi fotovoltaici-termici (PV/T) per la produzione combinata di energia elettrica e calore.

Tre prototipi di dispositivi PV/T sono stati caratterizzati sperimentalmente e confrontati tra loro. I prototipi consistono di un modulo in silicio cristallino e di una piastra canalizzata roll-bond in alluminio, che è applicata sul retro del modulo ed è utilizzata come scambiatore di calore. I tre dispositivi si differenziano per il modo in cui lo scambiatore di calore roll-bond è applicato al modulo.

Sono state eseguite misure di efficienza elettrica e termica dei dispositivi PV/T. I risultati dell'indagine sperimentale sono stati utilizzati per la validazione di un nuovo modello numerico per la caratterizzazione delle prestazioni termiche ed elettriche di dispositivi PV/T. Il modello può rappresentare un valido strumento per studiare i parametri su cui agire per aumentare l'efficienza e calcolare la producibilità elettrica del dispositivo.

Le curve di efficienza elettrica e termica sono state quindi impiegate per calcolare la producibilità annua di energia elettrica e calore di un dispositivo PV/T, a partire da un database di radiazione solare e temperatura ambiente. Sono riportati i risultati di alcune simulazioni riguardanti l'utilizzo di dispositivi PV/T in Italia.